Cancer Chemother Pharmacol (2003) 51: 107–118
DOI 10.1007/s00280-002-0542-3

ORIGINAL ARTICLE

**Sophie Callies · Dinesh P. de Alwis · James G. Wright
Alan Sandler · Michael Burgess · Leon Aarons**

A population pharmacokinetic model for doxorubicin and doxorubicinol in the presence of a novel MDR modulator, zosuquidar trihydrochloride (LY335979)

Received: 19 June 2002 / Accepted: 10 October 2002 / Published online: 10 January 2003

Abstract *Purpose*: To develop a population pharmacokinetic model for doxorubicin and doxorubicinol in the presence of zosuquidar.3HCl, a potent P-glycoprotein inhibitor. *Methods*: The population approach was used (implemented with NONMEM) to analyse doxorubicin-doxorubicinol pharmacokinetic data from 40 patients who had received zosuquidar.3HCl and doxorubicin intravenously (separately in cycle 1 and concomitantly in cycle 2 over 48 h and 0.5 h, respectively). *Results*: A five-compartment pharmacokinetic model (including three compartments for doxorubicin pharmacokinetics with two pathways for doxorubicinol formation) best described the doxorubicin-doxorubicinol pharmacokinetics in the presence of zosuquidar.3HCl. Doxorubicin clearance (CL), peripheral volume of distribution (V2) and doxorubicinol apparent clearance (CLm/fm) and apparent volume of distribution (Vm/fm) were 62.3 l/h, 2360 l, 143 l/h and 3150 l, respectively, in the absence or presence of low doses of zosuquidar.3HCl (<500 mg). In the presence of high doses of zosuquidar.3HCl ($\geq$500 mg), these values decreased by 25%, 26%, 48% and 73%, respectively, and doxorubicinol pharmacokinetics were characterized by a delayed t_{max} (24 h versus 4 h), which led to the inclusion of the parallel pathways. A decrease in the objective function ($P<0.005$) was observed when the impact of zosuquidar.3HCl was accounted for. *Conclusions*: This integrated parent-metabolite population pharmacokinetic model accurately characterized the increase in doxorubicin and doxorubicinol exposure (1.33- and 2-fold, respectively) in the presence of zosuquidar.3HCl ($\geq$500 mg) and provided insights into the pharmacokinetic interaction, which may be useful in designing future clinical trials.

Keywords LY335979 · Doxorubicin · Doxorubicinol · Pharmacokinetics · NONMEM

S. Callies · L. Aarons
School of Pharmacy and Pharmaceutical Sciences,
University of Manchester,
Manchester M13 9PL, UK

D.P. de Alwis (✉) · J.G. Wright · M. Burgess
Eli Lilly and Company Ltd,
Erlwood Manor, Sunninghill Road,
Windlesham, Surrey GU20 6PH, UK
E-mail: DEALWIS_Dinesh@Lilly.com
Tel.: +44-1276-483509
Fax: +44-1276-483588

A. Sandler
Vanderbilt University Medical Center,
2201 West End Avenue,
Nashville, TN 37235, USA

Introduction

Multidrug resistance (MDR), the ability of cancer cells to become resistant to chemotherapeutic agents that are structurally and functionally unrelated, may be caused by a variety of factors [2, 3, 13, 20, 23, 44]. One of the most prevalent forms of MDR is associated with overexpression of membrane transport proteins, for example P-glycoprotein (P-gp) [21, 33] and multidrug resistance-associated proteins (MRPs).

One strategy to overcome MDR is the use of non-cytotoxic small molecules that inhibit the efflux activity of the MDR transport proteins. Second- and third-generation MDR modulators are already in clinical development. These compounds bind with high affinity to P-gp and demonstrate potent in vitro reversal activity against MDR human tumour cell lines [23]. Some examples include PSC-833 [15, 22, 24, 38], R-verapamil [27], S9788 [27, 32, 45], GF120918 [14, 18, 40], MS-209 [14, 28], KR-30035 [26], XR9576 [41] and VX-710 [29]. An important outcome of clinical trials investigating the safety of doxorubicin (DOX) or paclitaxel administered alone and concomitantly with PSC833 [1, 6, 15], GF120919 [40] or VX-710 [29, 34] is the important but expected pharmacokinetic interaction [23] characterized by a decrease in the clearance of the anticancer drug (hence an increase in exposure).

Zosuquidar.3HCl [8, 10] (LY335979 or LY) is a novel third-generation MDR modulator that was first identified by its ability to restore DOX sensitivity to P-gp-expressing cell lines, enhancing the survival time of mice inoculated with P388/ADR cells. In vitro experiments have shown that zosuquidar.3HCl inhibits P-gp with a K_i of 59 n*M* (displacement of vinblastine in equilibrium-binding studies), does not inhibit either MRP1 or MRP2 and has no affinity for the liver enzymes CYP3A, CYP1A, CYP2C9, CYP2D6 at nanomolar levels [8, 9, 10, 16, 36, 48]. Lack of pharmacokinetic interactions with zosuquidar.3HCl should permit normal doses of chemotherapy to be administered and allow more straightforward interpretation of clinical trial results. The pharmacokinetic data collected were fitted using a population approach in order to describe and predict DOX and doxorubicinol (DOXOL) pharmacokinetics in the presence and absence of zosuquidar.3HCl.

Methods

Patient selection

Patients with a histological or cytological diagnosis of metastatic or locally advanced cancer who had failed conventional therapy, had disease considered refractory to standard chemotherapy regimens, or had disease for which no standard chemotherapy was available, were entered into the study. All participants gave written informed consent and the study was conducted in accordance with the ethical principles of the most recent version of the Declaration of Helsinki. Patients were at least 18 years of age, and met other eligibility requirements which included having a resting blood pool heart scan with an ejection fraction of greater than 45%, a performance status of 0 to 2 on the Eastern Cooperative Oncology Group scale, and an estimated life expectancy of at least 16 weeks. A patient's lifetime cumulative anthracycline dose (PLCAD) was not to exceed the DOX equivalent of 300 mg/m^2 in order that the PLCAD at the end of this clinical trial would remain below 500–550 mg/m^2 (the threshold value above which cardiomyopathy is observed). Adequate organ function (bone marrow, liver and kidney) was required. A description (demographic and laboratory values) of the patient population enrolled in this study is presented in Table 1.

Study design and treatment

Entered into this study were 40 patients in cohorts of three. The patients received zosuquidar.3HCl as a 48-h continuous intravenous infusion and DOX as a 0.5-h intravenous infusion separately and concomitantly in cycles 1 and 2, respectively. The dose administration scheme for each cohort is given in Table 2 (each patient received the same dose of each compound in cycle 1 and cycle 2). In cycle 1, zosuquidar.3HCl was administered on days 1 and 2 and DOX was administered on day 15. In cycle 2 (35 days after the beginning of cycle 1), DOX administration began 24 h (day 2 of the cycle) after the start of the zosuquidar.3HCl 48-h infusion.

Pharmacokinetic data and biological assays

Plasma samples were collected to determine the pharmacokinetics of zosuquidar.3HCl, DOX and DOXOL according to the schedule presented Table 3. Zosuquidar.3HCl concentrations were determined using a reverse-phase HPLC method validated in the range 20–2000 ng/ml with fluorescence detection in human plasma (excitation and emission wavelengths 240 and 415 nm, respectively). DOX and DOXOL concentrations were determined using a HPLC method validated in the range 0.5 ng/ml (precision 7.09%) to 100 ng/ml with fluorescence detection (excitation and emission

Table 1 Demographic and biological characteristics of the patients enrolled (cycle 1). Data are expressed as median (range), except number of patients

Covariates (unit)	Values
Men	18
Women	18
Smokers	9
Nonsmokers	27
Age (years)	57 (27–73)
Serum albumin (g/dl)	3.5 (2.3–4.7)
Alkaline phosphatase (U/l)	92 (47–592)
Alanine aminotransaminase (U/l)	19 (7–12.9)
Aspartate aminotransaminase (U/l)	20 (8–106)
Total bilirubin (mg/dl)	0.3 (0.2–0.7)
Body mass index (kg/m^2)	27.5 (18.2–39.7)
Body surface area (m^2)	1.99 (1.37–2.69)
Chloride plasma level (meq/l)	103 (96–110)
Creatinine clearance (ml/min)[a]	108.1 (55.5–291.7)
Haemoglobin (g/dl)	11.4 (8.7–15.7)
Height (cm)	172 (150–198)
Phosphate plasma (mg/dl)	3.8 (2.3–4.6)
Potassium plasma (meq/l)	4.2 (3.0–5.6)
Plasma protein (g/dl)	6.8 (5.9–8.0)
Red blood cells ($\times 10^{12}$/l)	3.96 (2.98–5.07)
Serum creatinine (mg/dl)	0.7 (0.4–1.6)
Sodium plasma (meq/l)	140 (131–147)
White blood cells ($\times 10^9$/l)	7.09 (2.70–14.60)
Weight (kg)	82.7 (43.1–137.0)

[a]Based on the Cockcroft and Gault equation (X = 72 for males and 85 for females): $\mathrm{CrCL(ml/min)} = \frac{[(140-\text{current age(years)})*(\text{weight})(\text{kg}))]}{X*\text{serum creatinine concentration (mg/dL)}}$

Table 2 Dose administration scheme for each cohort. The discrepancies between the number of patients having received a dose and the number of patients whose data were used in the pharmacokinetic analysis and between cycle 1 and cycle 2 (cohorts 7 and 9) are because a few patients did not complete the study (stopped after the first administration of zosuquidar.3HCl and did not receive any dose of DOX or stopped after completion of cycle 1)

	Dose (mg/m^2)		Number of patients	
	Zosuquidar.3HCl	DOX	Cycle 1	Cycle 2
Cohort 1	40	45	3	3
Cohort 2	40	60	3	3
Cohort 3	80	60	3	3
Cohort 4	160	60	3	3
Cohort 5	320	60	3	3
Cohort 6	640	60	3	3
Cohort 7	1280	60	6	5
Cohort 8	1280	75	3	3
Cohort 9	960[a]	75	13	6
Patients receiving a dose			40	32
Patients whose data were used for pharmacokinetic analysis			36	32

[a]Except patient 29 cycle 1 1280 mg/m^2

Table 3 Sampling schedule

Time from beginning of infusion (h)		Blood samples taken (X)	
Zosuquidar. 3HCl	DOX	Zosuquidar. 3HCl	DOX and DOXOL
0 (predose)		X	No sampling
2		X	No sampling
6		X	No sampling
12		X	No sampling
24	Predose	X	X
24.5	0.5	No sampling	X
25	1	No sampling	X
25.5	1.5	No sampling	X
26	2	No sampling	X
28	4	No sampling	X
30	6	No sampling	X
33	9	No sampling	X (only in cycle 1)
36	12	X	X (only in cycle 2)
48	24	X	X
48.5		X	No sampling
49		X	No sampling
49.5		X	No sampling
50		X	No sampling
52		X	No sampling
54	30	X	X (only in cycle 1)
72	48	X	X
96	75	X	X
120	96	No sampling	X

wavelengths 470 and 550 nm, respectively), which had been adjusted (2.5 to 1000 ng/ml) to minimize the number of dilutions required by the high concentrations in patient samples. Based on quality control samples, the overall relative standard deviation (expression of precision) was less than 12.8% and 9% for zosuquidar.3HCl and DOX-DOXOL, respectively. The overall relative error (expression of accuracy) was less than 2.0% and 6.0% for zosuquidar.3HCl and DOX-DOXOL, respectively.

Data analysis

The population pharmacokinetic model for DOX was defined, and the corresponding final pharmacokinetic parameters (means and variances from the model included the impact of zosuquidar.3HCl on DOX pharmacokinetic parameters), were fixed during the development of the DOXOL pharmacokinetic model. All analyses were performed with NONMEM (version V) using the first-order conditional method with interaction [4, 37, 42, 49].

First, a basic pharmacokinetic model, defined as describing adequately the mean population and individual tendencies without inclusion of any covariates, was determined. The structure for the random effects was as follows: (a) the departure of individual pharmacokinetic parameters estimates from the corresponding population mean estimate (interindividual variability, IIV, and interoccasion variability, IOV) was modelled according to an exponential relationship; (b) additive, proportional and combined (additive plus proportional) relationships were tested to model the departure of the model predictions from the observations (residual variability) [46]. At this stage the impact of Zosuquidar.3HCl on DOX and DOXOL pharmacokinetics was investigated and tested in NONMEM.

Second, to select other important covariates and the functional relationships between those covariates and the pharmacokinetic parameters, a stepwise generalized additive model (GAM) based on individual pharmacokinetic parameter estimates from the basic population model as dependent variables was performed outside NONMEM with the Xpose program [20]. The resulting covariate-pharmacokinetic parameter relationships were tested for statistical significance with NONMEM according to the selection criterion described by Troconiz et al. [46]. The covariance among the random effects was also explored at this stage of the analysis.

Model selection was based on the goodness of fit plots, the estimates and the confidence intervals of the fixed and random parameters, and the minimum value of the objective function. Finally, based on pharmacokinetic parameters from the final model, 1000 simulations were carried out using the Monte-Carlo method in order to generate the population 95% prediction interval. Also, a simultaneous estimation of DOX and DOXOL pharmacokinetic parameters was attempted at this stage of the analysis.

Population pharmacokinetic analysis of zosuquidar.3HCl was carried out but was not the objective of this study. Hence, in addition zosuquidar.3HCl absolute dose, the AUC and C_{max} (the area under the concentration versus time curve and the observed maximal concentration, respectively) could be used to study the effect of zosuquidar.3HCl on DOX and DOXOL pharmacokinetics.

Results

DOX pharmacokinetics, were adequately described by a three-compartment pharmacokinetic model (Fig. 1a, b). The basic pharmacokinetic model for DOX included IIV and IOV terms on the following fixed-effect parameters: the total plasma clearance (CL), the intercompartmental clearance (Q2), and the peripheral volume of distribution (V2). Residual variability was modelled using a proportional error. Due to the wide range of DOX plasma concentrations, the logarithm of the concentrations was modelled. The goodness of fit plots (Fig. 1c) for the final DOX model clearly showed no trends.

Figure 2a, b shows the post hoc individual estimates (from the basic model) of DOX CL and V2 in the presence versus the absence of zosuquidar.3HCl. Although it can be observed that low doses of zosuquidar.3HCl (< 500 mg total dose equivalent to 300 mg/m^2, cohort 5 and below) did not seem to affect the estimate of CL and V2, CL seems to be lower in the presence of greater exposure to zosuquidar.3HCl (Fig. 2a, c). A categorical model (cut-off value estimated at 500 mg zosuquidar.3HCl) and a sigmoidal E_{max} model were tested to describe this relationship. These two models gave very similar results (pharmacokinetic parameter mean and variance, decrease in the objective function minimum value, see Table 4). As the pharmacokinetics of zosuquidar.3HCl are linear, one can also use as a suitable cut-off the corresponding C_{max} and AUC instead of the dose (Table 5). The range of zosuquidar.3HCl C_{max} and AUC for zosuquidar.3HCl doses greater than 500 mg were 195–951.2 μg/l and 9115–42789 μg·h/l, respectively. The overall means ± SD of zosuquidar.3HCL C_{max} and AUC normalized to a dose of 500 mg were 121 ± 40.2 μg/l and 5944 ± 1746 μg·h/l, respectively (these values are similar to the EF_{50} values listed in Table 4). The categorical model (Table 4) was chosen as a pragmatic clinical model and because the data were too sparse to describe accurately the declining phase of the sigmoidal E_{max} relationship. The model predicts reductions in CL and V2 of 25.2% and

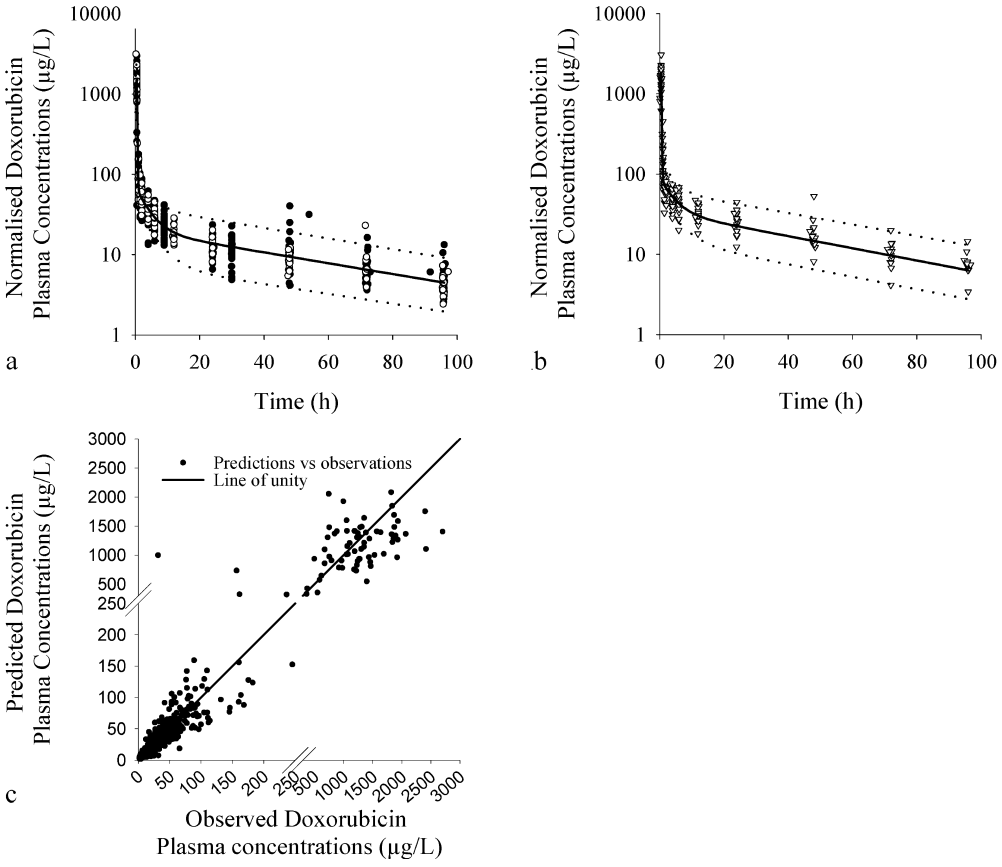

Fig. 1a–c DOX observed and predicted (*solid line* mean, *dotted line* 95% prediction interval) plasma concentrations versus time profiles following a 30-min intravenous administration of 75 mg/m^2 of DOX (**a**) in the absence (*solid circles*) or presence of zosuquidar.3HCl at doses < 500 mg (*open circles*) and (**b**) in the presence of zosuquidar.3HCl at doses ≥500 mg (*open triangles*). **c** Model goodness of fit plots

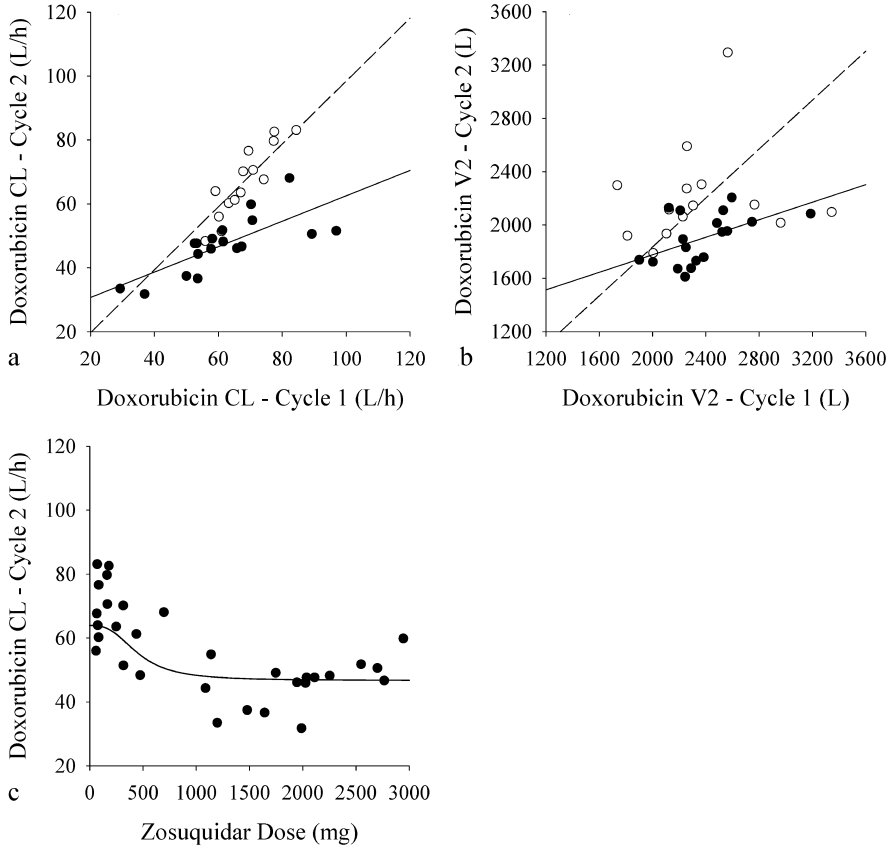

Fig. 2a–c Relationships between DOX pharmacokinetic parameters (CL and V2) and zosuquidar.3HCl dose. **a**, **b** Categorical model with patients who received zosuquidar.3HCl at doses < 500 mg (*open circles*, *dashed line* regression line) and at doses ≥500 mg (*closed circles*, *solid line* regression line). **c** Sigmoidal E_{max} model

Table 4 DOX population pharmacokinetic parameters (*CL* total clearance; *Q2*, *Q3* intercompartmental clearances; *V1*, *V2*, *V3* central and peripheral volumes of distribution)

		Basic model		Categorical relationship (final model)		Continuous relationship	
		Value	SE (%)	Value	SE (%)	Value	SE (%)
Objective function		–1073.326		–1127.957		–1133.386	
CL (l/h)		57.6	4.91	62.3[a]	5.01	62.8[a]	5.03
Effect of zosuquidar.3HCl	Decrease when dose ≥500 mg (%)	–	–	25.2	12.3	–	–
	E_{max} decrease from baseline (%)	–	–	–	–	25.5	14.5
	Zosuquidar.3HCl $dose_{50}$ (mg)	–	–	–	–	420	21.1
	γ_2	–	–	–	–	3.49	49.6
V2 (l)		2170	5.81	2360[a]	14.5	2390[a]	6.36
Effect of zosuquidar.3HCl	Decrease when dose ≥500 mg (%)			26.2	14.5	–	–
	E_{max} decrease from baseline (%)					28.0	16.5
	Zosuquidar.3HCl $dose_{50}$ (mg)					420	21.1
	γ_2					3.49	49.6
V1 (l)		21.2	8.11	21.5	8.56	21.5	8.70
Q2 (l/h)		84.7	9.70	85.8	10.4	85.9	10.6
Q3 (l/h)		34.7	10.9	35.6	11.7	35.6	12.0
V3 (l)		101	12.1	104	13.6	104	14.4
Interindividual variability (%)[b]							
CL		20.5	36.0	20.5	34.4	20.3	36.4
Q2		10.6	66.5	10.3	151	6.86	796
V2		7.30	70.7	13.6	76.1	14.4	61.7
Interoccasion variability (%)[b]							
CL		17.9	28.4	8.36	62.5	7.94	70.2
V2		26.0	21.6	18.5	64.5	16.8	69.8
Q2		50.8	102	50.1	129	50.4	138
Residual error Proportional error (%)		22.4	17.3	22.5	17.4	22.5	17.4

[a]Pharmacokinetic values in the absence or presence of zosuquidar.3HCl at doses ≤ 500 mg

[b]Interindividual and interoccasion variability on different pharmacokinetic parameters expressed as coefficients of variation in percent. The SE values for these parameters are the values on the corresponding variance term calculated by NONMEM ($CV = 100 \times (\text{variance})^{0.5}/\text{mean}$). The off-diagonal terms (covariances ωCL-V2, ωCL-Q2 and ωQ2-V2) were tested but did not improve the model (very small values)

26.2%, respectively, with zosuquidar.3HCl at doses ≥500 mg.

DOXOL concentration versus time profiles showed differences (increase in AUC, delayed t_{max}) when the total dose of zosuquidar.3HCl was greater than 500 mg (Fig. 3a, b). A model with five compartments best accounted for these differences (Fig. 3c, d). The DOX pharmacokinetic model being the input function for the DOXOL pharmacokinetic model, a fourth compartment (DOXOL compartment) was linked to the DOX central compartment. This model adequately predicted the DOXOL pharmacokinetic profile, in the absence or presence of low doses (< 500 mg) of zosuquidar.3HCl (Fig. 4, left and middle graphs). DOXOL parameters were expressed as apparent clearance (CLm/fm, where fm is the fraction of DOX converted to DOXOL) and apparent volume of distribution (Vm/fm). In the presence of zosuquidar.3HCl at doses ≥500 mg, a fifth compartment was added between the DOX central compartment and the DOXOL compartment (Fig. 3d). Consequently, the DOX output pharmacokinetic was divided into two routes, both of them leading to the DOXOL compartment, and therefore defining a parallel

Table 5 Correspondence between the parameters of a categorical and sigmoidal E_{max} model describing the impact of zosuquidar.3HCl on DOX pharmacokinetics: cut-off and EF_{50} values (EF_{50} zosuquidar.3HCl total dose, C_{max} and AUC which lead to 50% of the maximal decrease in DOX clearance and volume of distribution when DOX is administered with zosuquidar.3HCl)

Zosuquidar.3HCl	Cut-off	EF_{50}
Dose (mg)	500	420
C_{max} (μg/l)	200	133
AUC (μg·h/l)	5000	5900

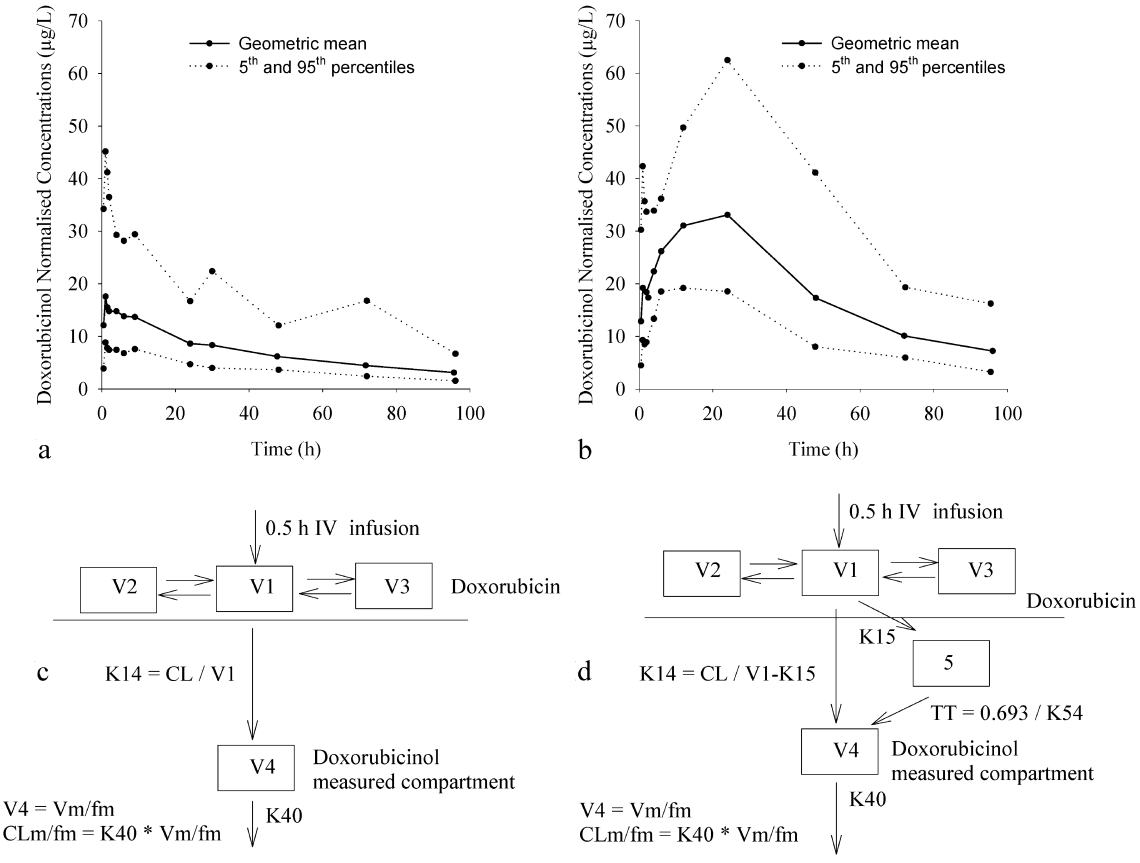

Fig. 3a–d DOXOL typical pharmacokinetic profiles (**a**) in the absence and presence of zosuquidar.3HCl at doses < 500 mg and (**b**) in the presence of zosuquidar.3HCl at doses ≥500 mg. **c**, **d** Corresponding pharmacokinetics models

input pharmacokinetic model for DOXOL. The fifth compartment (two additional parameters) helped to characterize the later t_{max} (24 h versus 4 h, median t_{max} in cycle 1) observed in the DOXOL pharmacokinetic

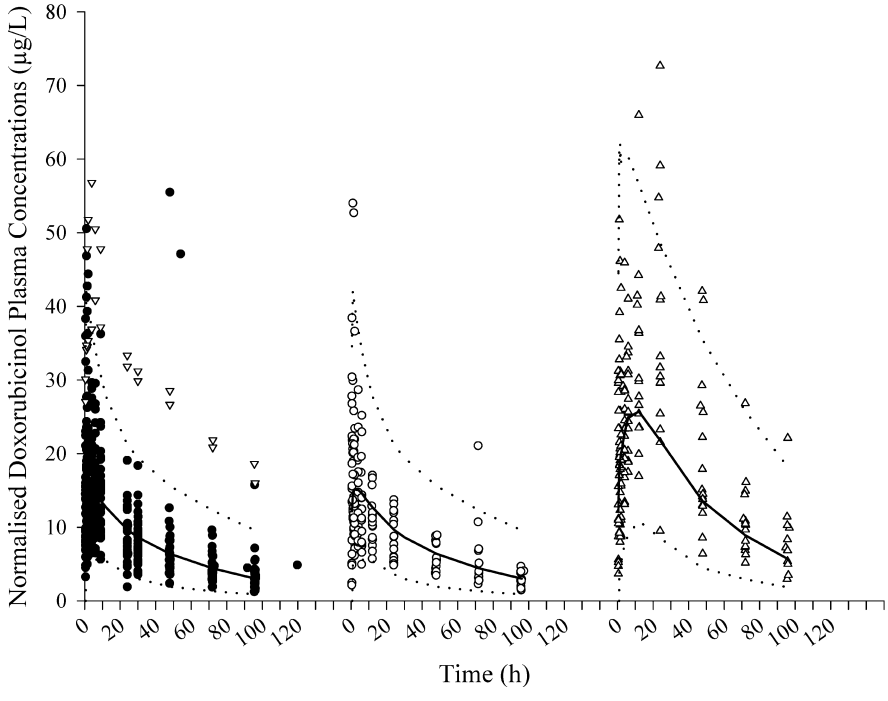

Fig. 4 DOXOL observed and predicted (*solid line* mean, *dotted line* 95% prediction interval) plasma concentrations versus time profiles following a 30-min intravenous administration of 75 mg/m^2 of DOX in the absence of zosuquidar.3HCl (*left graph*, *closed circles*; *open triangles* patients 33 and 35) and the presence of zosuquidar.3HCl at doses < 500 mg (*middle graph*) or ≥500 mg (*right graph*)

profile with zosuquidar.3HCl at doses ≥500 mg and led to a significant ($P < 0.005$) improvement of the model.

The residual error model for DOXOL was a proportional error model with an additional additive component when time after dose was less then 1 h. This residual error model was chosen because, between 0 and 1 h after administration, the prediction of the DOXOL pharmacokinetic input function (that is DOX pharmacokinetics) was supported only by two observations per patient and was particularly dependent on the accuracy in recording the sampling time (DOX concentrations decrease very rapidly between 0 and 1 h after administration). This additive component was added in order to overcome the consequences of inaccuracy in the prediction of DOX pharmacokinetics (in the early distribution phase) on the prediction of DOXOL pharmacokinetics and to give more flexibility for the program to estimate DOXOL exposure. This model adequately predicted the DOXOL pharmacokinetics in the presence of zosuquidar.3HCl at doses ≥500 mg, which were characterized by an increase in AUC (1.82 ± 0.90-fold increase, $n = 18$; from 790 to 1466 μg·h/l following 75 mg/m^2 DOX; Fig. 4, right graph). The inclusion in the model of the impact of zosuquidar.3HCl on DOX and DOXOL pharmacokinetics led to a significant decrease in the minimum value of the objective function ($P < 0.005$) and in the IOVs CL, V2, CLm/fm and Vm/fm.

The impact of zosuquidar.3HCl on DOX-DOXOL pharmacokinetics being accounted for, the GAM analysis was carried out to select other potential important covariates. The results were as follows: (a) gender, albumin (ALB) and bilirubin (BIL) levels, the aspartate transaminase activity (AST) and the creatinine clearance (CRCL) on CL; (b) weight (WGT) and CRCL on V2; and (c) gender on CLm/fm and Vm/fm, AST on Vm/fm, CRCL, BIL and DOX absolute dose on CLm/fm. When these covariate effects were tested in NONMEM, only BIL and AST on DOXOL pharmacokinetic parameters were significant. However, these relationships were driven by data from two patients (patients 33 and 35) and therefore were not thought to be robust enough to be retained in the model (see Fig. 5b vs a). The covariate values (other than BIL and AST) for these two patients were similar to the values observed for the rest of the population. The DOXOL population pharmacokinetic parameters are presented Table 6 and the control stream of this final DOX-DOXOL model is presented in Appendix 1.

Discussion

The pharmacokinetics of the anthracycline, DOX, have been well documented [7, 17, 19, 25, 30, 31, 43]. The cumulative biliary excretion of DOX is estimated to be approximately 40% of the dose. The aldoketoreductase enzyme system (responsible for the formation of the major metabolite, DOXOL) is present in all cells, but particularly white and red blood cells, and liver and kidney cells. DOXOL is eliminated by biliary excretion, but limited quantities may also be recovered in the urine [17]. Both P-gp and MRPs are involved in the excretion of DOX and DOXOL [5]. DOXOL possesses approximately 10% of the activity of DOX [35] but is reported to play a key role in mediating the cardiotoxicity seen after DOX administration [50].

The five-compartment pharmacokinetic model for DOX-DOXOL adequately described the data. The model predicted a decrease in both CL and CLm/fm (25.2% and 47.8%, respectively) in the presence of zosuquidar.3HCl at total doses > 500 mg. In addition the t_{max} of DOXOL was delayed (24 h versus 4 h) and corresponded to the end of zosuquidar.3HCl infusion. The model was based on the following hypothesis. When a certain exposure of zosuquidar.3HCl is reached, a critical degree of P-gp inhibition at the cellular level results. This, in turn, prevents the P-gp-mediated efflux of both parent and metabolite from cells. The principle site of metabolism and excretion for DOX being the liver, the pharmacokinetic processes following DOX infusion and the impact of zosuquidar.3HCl can be

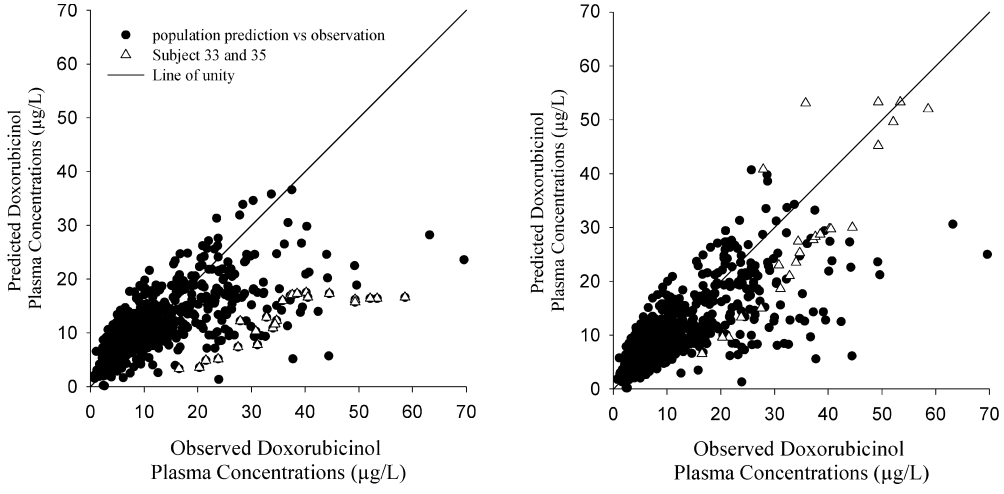

Fig. 5a, b DOXOL model goodness of fit plots (**a** model without AST and BIL, **b** model with these covariates, *open triangles* patients 33 and 35)

Table 6 DOXOL population pharmacokinetic parameters (*CLm/fm* apparent clearance; *Vm/fm* apparent volume of distribution; *K15*, *K54* rate constants of transfer from compartment 1 to 5 and from 5 to 4, respectively)

	Value	SE (%)
CLm/fm (l/h)[a]	143	8.88
Effect of zosuquidar.3HCl at doses ≥500 mg (% decrease)	47.8	9.23
Vm/fm (l)	3150[a]	9.81
Effect of zosuquidar.3HCl at doses ≥500 mg (l)	855[b]	9.64
K15 (h^{-1})	0 (fixed)	–
Effect of zosuquidar.3HCl at doses ≥500 mg (l/h)	1.30	6.92
TT (h)[c]	0 (fixed)	–
Effect of zosuquidar.3HCl at doses ≥500 mg (h)	7.04	8.31
Interindividual variability (%)[d]		
CLm/fm	41.6	39.4
Vm/fm	47.7	43.3
Interoccasion variability (%)[d]		
CLm/fm	28.3	47.0
Vm/fm	33.6	100
Residual error		
Proportional error (%)	18.7	7.81
Additive error (time after dose 0–1 h) (μ/l)	5.77	14.0

[a]In the absence of zosuquidar.3HCl or in the presence of zosuquidar.3HCl at doses < 500 mg

[b]72.9% decrease in Vm/fm in the presence of zosuquidar.3HCl at doses ≥500 mg

[c]Half-life corresponding to the delayed rate constant K54 (= 0.693/K54)

[d]Interindividual and interoccasion variability on different pharmacokinetic parameters expressed as coefficients of variation in percent. The SE values for these parameters are the SE values on the corresponding variance term calculated by NONMEM ($CV = 100 \times (\text{variance})^{0.5}/\text{mean}$)

summarized as in Fig. 6. The decrease in both parent and metabolite CL could readily be explained by a reduction in P-gp-mediated efflux at the level of the bile canaliculi.

If this hypothesis is correct, then the delay in DOXOL t_{max} and the reduction in CL and CLm/fm should continue as long as P-gp inhibition remains above this threshold. After this, P-gp activity should gradually return to normal as zosuquidar.3HCl concentration drops and the substrates (DOX-DOXOL) are again effectively effluxed from the cells. In this study, zosuquidar.3HCl infusion was maintained for 24 h following DOX administration during which time the zosuquidar.3HCl concentration remained above the threshold (200 μg/l) and P-gp inhibition was sustained. As zosuquidar.3HCl has a rapid distribution phase [11], zosuquidar.3HCl plasma concentrations fall rapidly after the infusion is stopped, reversing the P-gp inhibition. The t_{max} (24 h) of DOXOL effectively corresponds to this time.

The presence of two peaks in DOXOL in some patients but not in others is a potential difficulty, and has also been previously reported in the literature [19]. This may be associated with distribution and/or clearance of DOXOL from plasma following an initial rapid metabolism of DOX in the central compartment. Based on the data available from this study, it was not possible to characterize or fully explore this hypothesis. This could be further investigated when more DOX and DOXOL data become available from future studies.

Although the model presented is empirical, there is a mechanistic basis to it. The purpose of the fifth compartment is to allow for a delay between DOXOL input pharmacokinetics and output pharmacokinetics and to act as a "depot" compartment mimicking the hypothesis that P-gp inhibition prevents DOXOL clearance. Hence DOXOL plasma concentrations increase toward an equilibrium state until P-gp inhibition is stopped. The short distribution half-life of zosuquidar.3HCl and the

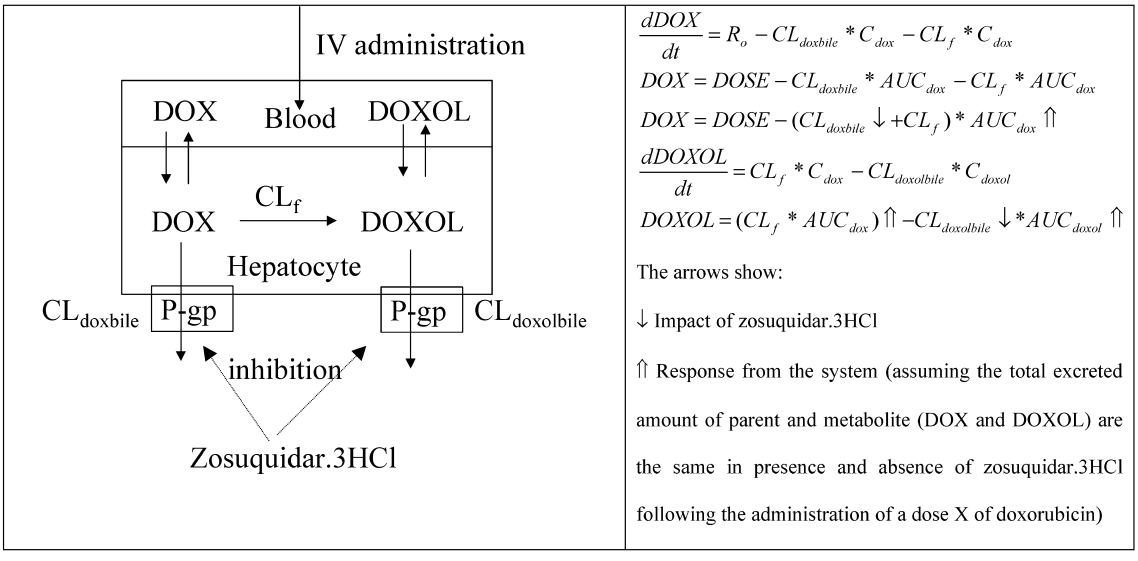

Fig. 6 Hypothesis to explain the increase in DOX and DOXOL AUC in the presence of P-gp inhibition and corresponding differential equations

direct pharmacokinetic/pharmacodynamic relationship (between the percent inhibition of P-gp activity in CD56 cells and zosuquidar.3HCl concentration) support the hypothesis that the decrease in DOXOL concentration after 24 h occurs because of the end of P-gp inhibition (zosuquidar.3HCl concentrations fall rapidly at the end of infusion, reversing P-gp inhibition and allowing DOXOL clearance).

Trials with other MDR modulators (PSC-833, GF120918, XR9576) [12, 15, 40] combined with DOX have shown larger increases in AUC and C_{max} than were demonstrated with zosuquidar.3HCl in this study. This could be attributed to the specificity of zosuquidar.3HCl for P-gp compared to non-P-gp transporters. Since DOX is transported by both P-gp and MRP, the impact of a less-specific modulator (PSC-833) will be greater (tenfold increase in DOXOL AUC) [15]. Additionally the impact on DOXOL AUC, as described above, is influenced significantly by the period of P-gp inhibition. In the studies with PSC-833 and GF120918 this period following DOX infusion was significantly longer (72 h) [15, 40]. In the same way, drugs with a prolonged half-life (e.g. XR9579 with a half-life of 40.8 h) will produce similar results [12]. The impact of both specificity and duration of inhibition will have a bearing on the toxicity of DOX. Sparreboom et al. [40] highlight DOXOL exposure as the major determinant of DOX-mediated toxicity. Consequently, factors which increase DOXOL exposure will also encourage dose-limiting toxicity. This may be evident in the presence of these inhibitors. Hence in these trials (with PSC-833 and GF120918) the maximum tolerated dose of DOX was 50 mg/m^2 or less, in contrast to 75 mg/m^2 with zosuquidar.3HCl found in this study.

There was a greater increase in the AUC ratio of DOXOL (2-fold, increase in AUC from 790 to 1466 μg·h/l following 75 mg/m^2 DOX) compared to the AUC ratio for DOX (1.3-fold, increase in AUC from 2065 to 2767 μg·h/l following 75 mg/m^2 DOX) when given in combination with zosuquidar.3HCl. The mechanism for this remains unknown. One hypothesis may be that inhibition of P-gp affects DOXOL to a greater degree than DOX. This could be achieved by an increased amount of DOX trapped in the hepatocytes (as a consequence of P-gp inhibition) being converted to the metabolite (DOXOL fm would increase). Figure 6 illustrates that, even if P-gp inhibition affects DOX and DOXOL equally, a greater increase in DOXOL AUC compared to that of DOX would be expected. An alternative hypothesis is that a greater percentage of parent than metabolite is excreted via non-P-gp transporter.

The mechanisms responsible for the decreased volume of distribution at steady state ($V_{ss} = V1 + V2 + V3$) of DOX in the presence of zosuquidar.3HCl remain unclear. The overall mean DOX V_{ss} in the absence of zosuquidar.3HCl was 2486 l, indicating that it is many times that of total body water. DOX has an extremely high affinity for its intracellular target, DNA, and this leads to sequestration of DOX in cell nuclei. P-gp acts against DOX tissue distribution by effluxing drug from cells, and therefore one could speculate that P-gp inhibition leads to greater cellular accumulation in tumours and normal tissue expressing P-gp. The change observed in V_{ss}, however, is not consistent with this effect. Recent studies have shown decreases in V_{ss} of P-gp substrates such as talinolol [39] and docetaxel [47] in the presence of P-gp inhibitors (verapamil and R101933, respectively). Another hypothesis could be that zosuquidar.3HCl gives rise to a decrease in tissue binding that would lead to a decrease in the volume of distribution. This is based on the fact that the apparent volume of distribution decreases when fraction unbound and total drug concentrations in tissue increase.

In this study, a 75 mg/m^2 dose of DOX administered with zosuquidar.3HCl (48 h) was well tolerated. However, six cycles of such a regimen cannot be administered safely because of the increase in DOX and DOXOL exposure. In the absence of zosuquidar.3HCl, six cycles of DOX 75 mg/m^2 (corresponding to a cumulative DOX dose of 450 mg/m^2, just below the toxic cumulative dose of 500–550 mg/m^2 leading to cardiomyopathy) led to cumulative AUCs for DOX and DOXOL of 12,390 μg·h/l and 4740 μg·h/l, respectively. In the presence of zosuquidar.3HCl at doses >500 mg (given according to the regimen of this study), the cardiotoxic cumulative exposure threshold based on DOXOL (4740 μg·h/l) would be achieved after three cycles, given that DOXOL AUC over one cycle in the presence of zozuquidar.3HCl at doses >500 mg is predicted to be 1466 μg·h/l.

Therefore, in future trials, the length and rate of the infusion of zosuquidar.3HCl need to be adjusted so that efficacious levels of zosuquidar.3HCl for optimal P-gp inhibition (higher than 200 μg/l) are obtained before the DOX infusion and maintained only during the distribution phase of DOX pharmacokinetics (3 to 4 h compared to the 24 h in this present study). This should prevent the efflux of DOX from the cancer cells when the drug is distributing in the tumours and therefore provide time for the drug to migrate in the cells and to bind to the cellular target (DNA). Once this is achieved there is no need to further maintain the P-gp inhibition. This adjustment should lead to a much lower impact on DOX-DOXOL pharmacokinetics, allowing the concomitant administration of DOX and zosuquidar.3HCl for six cycles.

The pharmacokinetic data collected in this study were used to develop a novel integrated DOX-DOXOL population pharmacokinetic model, which led to important insights into the pharmacokinetic interaction (described by a structural change in the model) between zosuquidar.3HCl, DOX and DOXOL.

Acknowledgements We wish to thank Christopher Sweeney, MD, and Michael Gordon, MD, for their expert clinical support in the conduct of this study. We are also grateful for the support of Indiana University School of Medicine.

Appendix 1. Control stream for the final DOX-DOXOL model

```
$PROBLEM doxorubicin-met pop pk
$INPUT ID CYC TIME AMT INF RATE DV EVID
CMT LYDO
$DATA dox_met.dta
$SUBROUTINE ADVAN5
$MODEL
NCOMPARTMENTS = 5
COMP (CENTRAL)
COMP (PERIPH1)
COMP (PERIPH2)
COMP (DELAY)
COMP (MET)
$PK
OCC3 = 0
OCC4 = 0
C1 = 0
C2 = 0
C4 = 0
IF (CYC.EQ.1) OCC3 = 1
IF (CYC.EQ.2) OCC4 = 1
IOV1 = OCC3*ETA(9) + OCC4*ETA(10)
IOV2 = OCC3*ETA(11) + OCC4*ETA(12)
IOV3 = OCC3*ETA(13) + OCC4*ETA(14)
IOV4 = OCC3*ETA(15) + OCC4*ETA(16)
IOV5 = OCC3*ETA(17) + OCC4*ETA(18)
IF (LYDO.GE.500) C1 = THETA(11)
IF (LYDO.GE.500) C2 = THETA(12)
IF (LYDO.GE.500) C4 = THETA(13)
TCL = THETA(1)*(1-C1)
CL = TCL*EXP(ETA(1) + IOV1)
V1 = THETA(2)*EXP(ETA(2))
Q2 = THETA(3)*EXP(ETA(3) + IOV3)
V2 = THETA(4)*(1-C2)*EXP(ETA(4) + IOV2)
Q3 = THETA(5)*EXP(ETA(5))
V3 = THETA(6)*EXP(ETA(6))
IF (LYDO.LT.500) THEN
K15 = 0
K14 = CL/V1
TV4 = THETA(8)
ELSE
K15 = THETA(15)
K14 = CL/V1-K15
TV4 = THETA(16)
END IF
TT = THETA(14)
K54 = LOG(2)/TT
TCLM = THETA(7)*(1-C4)
CLM = TCLM*EXP(ETA(8) + IOV4)
V4 = TV4*EXP(ETA(7) + IOV5)
S1 = V1/1000
S4 = V4/1000
K12 = Q2/V1
K21 = Q2/V2
K13 = Q3/V1
K31 = Q3/V3
K40 = CLM/V4
$ERROR
GROUP = 0
IF (TIME.LT.1) GROUP = 1
DEL = 0
IF (F.EQ.0) DEL = 1
W1 = 0
W2 = 0
IF (CMT.EQ.1) IPRED = LOG(F)
IF (CMT.EQ.4) IPRED = F
IF (CMT.EQ.1) W1 = 1
IF (CMT.EQ.4.AND.GROUP.EQ.1) W2 = SQRT (TH-
ETA(9)**2 + THETA(10)**2*IPRED**2)
IF (CMT.EQ.4.AND.GROUP.EQ.0) W2 = SQRT (TH-
ETA(10)**2*IPRED**2)
IRES = DV-IPRED
IWRES = IRES/(W1 + W2 + DEL)
Y = IPRED + W1*EPS(1) + W2*EPS(2)
$ESTIMATION METHOD = CONDITIONAL
INTERACTION NOABORT PRINT = 10 MAX-
EVALS = 9999
$COV
```

References

1. Advani R, Fisher GA, Lum BL, Hausdorff J, Halsey J, Litchman M, Sikic BI (2001) A phase I trial of doxorubicin, paclitaxel, and Valspodar (PSC833), a modulator of multidrug resistance. Clin Cancer Res 7:1221–1229
2. Ambukar SV, Dey S, Hrycyna CA, Ramachandra M, Pastan I, Gottesman MM (1999) Biochemical, cellular and pharmacological aspects of the multidrug transporter. Annu Rev Pharmacol Toxicol 39:361–368
3. Biedler JL, Riehm H (1970) Cellular resistance to actinomycin D in Chinese hamster cells in vitro: cross-resistance, radioautographic and cytogenetic studies. Cancer Res 30:1174–1184
4. Boeckmann AJ, Sheiner LB, Beal SL (1994) NONMEM users guide. NONMEM Project Group, University of California, San Francisco
5. Borst P, Evers R, Kool M, Wijnholds J (2000) A family of drug transporters: the multidrug resistance-associated proteins. J Natl Cancer Inst 92:1295–1302
6. Chico I, Kang MH, Bergan R, Abraham J, Bakke S, Meadows B, Rutt A, Robey R, Choyke P, Merino M, Goldspiel B, Smith T, Steinberg S, Figg WD, Fojo T, Bates S (2001) Phase I study of infusional paclitaxel in combination with the P-glycoprotein antagonist PSC833. J Clin Oncol 19:832–842
7. Chlebowsky RT, Brzechwa-Adjukiewicz A, Cowden A, Block JB, Tong M, Chan KK (1984) Doxorubicin (75 mg/m^2) for hepatocellular carcinoma: clinical and pharmacokinetic results. Cancer Treat Rep 68:487–491
8. Dantzig AH, Shepard RL, Cao J, Law KL, Ehlhardt WJ, Baughman TM, Bumol TF, Starling JJ (1996) Reversal of P-glycoprotein-mediated multidrug resistance by a potent cyclopropyldibenzosuberane modulator, LY335979. Cancer Res 56:4171–4179
9. Dantzig AH, Shepard RL, Law KL, Tabas L, Pratt S, Gillespie JS, Binkley SN, Kuhfeld MT, Starling JJ, Wrighton SA (1999) Selectivity of the multidrug resistance modulator, LY335979, for P-glycoprotein and effect on cytochrome P-450 activities. J Pharmacol Exp Ther 290:854–862
10. Dantzig AH, Law KL, Cao J, Starling JJ (2001) Reversal of multidrug resistance by the P-glycoprotein modulator LY335979, from the bench to the clinic. Curr Med Chem 8:39–50

11. De Alwis DP, Pouliquen I, Burgess M, Green L, Chaudhary A, Jordan C, et al (2001) A phase I dose escalating study of LY335979, a novel Pgp modulator – administered intravenously in combination with doxorubicin (abstract 284). Proc ASCO 20 (part 1)
12. Ferry D, Price L, Atsmon J, Inbar M, Merimsy O, Telligen O, et al (2001) A phase IIA pharmacokinetic and pharmacodynamic study of the P-glycoprotein inhibitor, XR9576, in patients treated with doxorubicin chemotherapy. Proc Am Assoc Cancer Res 42:950–5160
13. Ford JM, Hait WN (1990) Pharmacology of drugs that alter multidrug resistance in cancer. Pharmacol Rev 42:155–199
14. Germann UA, Ford PJ, Shlyakhter D, Mason VS, Harding MW (1997) Chemosensitization and drug accumulation effects of VX-170, verapamil, cyclosporin A, MS-209 and GF120918 in multidrug resistant HL60/ADR cells expressing the multidrug resistance-associated protein MRP. Anticancer Drugs 8:141–155
15. Giaccone G, Linn SC, Welink J, Catimel G, Stieltjes H, van der Vijgh WJF, Ecltink C, Vermorken JB, Pinedo HM (1997) A dose-finding and pharmacokinetic study of reversal of multidrug resistance with SDZ PSC 833 in combination with doxorubicin in patients with solid tumors. Clin Cancer Res 3:2005–2015
16. Green LJ, Marder P, Slapak CA (2001) Modulation by LY335979 of P-glycoprotein function in multidrug-resistant cell lines and human natural killer cells. Biochem Pharmacol 61:1393–1399
17. Grochow LB, Ames MM (1998) A clinician's guide to chemotherapy pharmacokinetics and pharmacodynamics, 1st edn. Williams & Wilkins, Baltimore, pp 93–122
18. Hyafil F, Vergely C, du Vignaud P, Grand-Perret T (1993) In vitro and in vivo reversal of multidrug resistance by GF120918, an acridonecarboxamide derivative. Cancer Res 53:4595–4602
19. Jacquet JM, Bressolle F, Galtier M, Bourrier M, Donadio D, Jourdan J, Rossi JF (1990) Doxorubicin and doxorubicinol: intra and inter-individual variation of PK parameters. Cancer Chemother Pharmacol 27:219–225
20. Jonson N, Karlsson M (1998) Xpose 2.0 user's manual. Department of Pharmacy, Uppsala University, Sweden
21. Juliano RL, Ling V (1976) A surface glycoprotein modulating drug permeability in chinese hamster ovary cell mutants. Biochim Biophys Acta 455:152–162
22. Krishna R, Mayer LD (1997) Liposomal doxorubicin circumvents PSC 833-free drug interactions, resulting in effective therapy of multidrug resistance solid tumor. Cancer Res 57:5246–5253
23. Krishna R, Mayer LD (2000) Multidrug resistance (MDR) in cancer; mechanisms, reversal using modulators of MDR and the role of MDR modulators in influencing the pharmacokinetics of anticancer drugs. Eur J Pharm Sci 11:265–283
24. Krishna R, St-Louis M, Mayer LD (2000) Increased intracellular drug accumulation and complete chemosensitization achieved in multidrug-resistant solid tumours by coadministering valspodar (PSC 833) with sterically stabilized liposomal doxorubicin. Int J Cancer 85:131–141
25. Leca F, Marchiset-Leca D, Noble A, Antonetti M (1991) New data on the pharmacokinetics of adriamycin and its major metabolite, adriamycinol. Eur J Drug Metab Pharmacokinet 16:107–111
26. Lee BH, Shin HS, Lee CO, Park SH, Yoo SE, Yi KY, Jung NP, Choi Su (2000) Effect of KR30035, a novel multidrug-resistance modulator, on the cardiovascular system of rat in vivo and on the cell cycle of human cancer cells in vitro. Anticancer Drugs 11:55–61
27. Massart C, Gibassier J, Raoul M, Pourquier P, Leclech G, Robert J, Lucas C (1995) Cyclosporin A, verapamil, and S9788 reverse doxorubicin resistance in human medullary thyroid carcinoma cell line. Anticancer Drugs 6:135–146
28. Nakanishi O, Baba M, Saito A, Yamashita T, Sato W, Abe H, Fukazawa N, Suzuki T, Sato S, Naito M, Tsuruo T (1997) Potentiation of the antitumor activity by a novel quinoline compound, MS-209, in multidrug-resistant solid tumor cell lines. Oncol Res 9:61–69
29. Peck RA, Hewett J, Harding MW, Wang YM, Chaturvedi PR, Bhatnagar A, Zeissman H, Atkins F, Hawkins MJ (2001) Phase I and pharmacokinetic study of the novel MDR1 and MRP1 inhibitor Biricodar administered alone and in combination with doxorubicin. J Clin Oncol 19:3130–3141
30. Piscitelli SC, Rodvold KA, Rushing DA, Tewksbury DA (1993) Pharmacokinetics and pharmacodynamics of doxorubicin in patients with small cell lung cancer. Clin Pharmacol Ther 53:555–561
31. Preiss R, Sohr R, Kittelman B, Muller E, Hasse D (1989) Investigations on the dose-dependent pharmacokinetics of adriamycin and its metabolites. Int J Clin Pharmacol Ther Toxicol 27:156–164
32. Punt CJ, Voest EE, Tueni E, Van Oosterom AT, Backx A, De Mulder PH, Hecquet B, Lucas C, Gerard B, Bleiberg H (1997) Phase IB study of doxorubicin in combination with the multidrug resistance reversing agent S9788 in advance colorectal and renal cancer. Br J Cancer 76:1376–1381
33. Rosenberg MF, Callaghan R, Ford RC, Higgins CF (1997) Structure of the multidrug resistance P-glycoprotein to 2.5 nm resolution determined by electron microscopy and image analysis. J Biol Chem 272:1065
34. Rowinsky EK, Smith L, Wang YM, Chaturvedi P, Villalona M, Campbell E, Aylesworth C, Eckhard SG, Hammond L, Kraynak M, Drengler R, Stephenson J, Harding MW, Von Hoff DD (1998) Phase I and pharmacokinetic study of paclitaxel in combination with biricodar, a novel agent that reverses multidrug resistance conferred by over expression of both MDR and MRP. J Clin Oncol 16:2964–2976
35. Schott B, Robert J (1989) Comparative activity of anthracycline 13-dihydrometabolites against rat glioblastoma cells in culture. Biochem Pharmacol 38:4069–4074
36. Schuetz EG, Beck WT, Schuetz JD (1996) Modulators and substrates of P-glycoprotein and cytochrome P4503A coordinately up-regulate these proteins in human colon carcinoma cells. Mol Pharmacol 49:311–318
37. Sheiner LB (1984) Population pharmacokinetics: the population approach to pharmacokinetic data analysis: rational and standard data analysis methods. Drug Metab Rev 15:153–171
38. Sonneveld P, Marie J, Huisman C (1996) Reversal of multidrug resistance by SDZ-PSC833, combined with VAD (vincristine, doxorubicin, dexamethasone) in refractory multiple myeloma. A phase I study. Leukemia 10:1741–1750
39. Spahn-langguth H, Baktir G, Radschuweit A, Okyar A, Terhaag B, Ader P, Hanafy A, Langguth P (1998) P-Glycoprotein transporters and the gastrointestinal tract: evaluation of the potential in vivo relevance of in vitro data employing talinolol as a model compound. Int J Clin Pharmacol Ther 36:16–24
40. Sparreboom A, Planting AST, Jewell RC, van der Burg ME, van der Gaast A, de Bruijn P, Loos WJ, Nooter K, Chandler LH, Paul EM, Wissel PS, Verweij J (1999) Clinical pharmacokinetics of doxorubicin in combination with GF120918, a potent inhibitor of MDR1 P-glycoprotein. Anticancer Drugs 10:719–728
41. Stewart A, Steiner J, Mellows G, Laguda B, Norris D, Bevan P (2000) Phase I trial of XR9576 in healthy volunteers demonstrates modulation of P-glycoprotein in CD56+ lymphocytes after oral and intravenous administration. Clin Cancer Res 6:4186–4191
42. Sun H, Fadiran EO, Jones CD, Lesko L, Huang S-M, Higgins K, Hu C, Machado S, Maldonado S, Williams R, Hossain M, Ette EI (1999) Population pharmacokinetics – a regulatory perspective. Clin Pharmacokinet 37:41–51
43. Sweatam TW, Lokich JJ, Israel M (1989) Clinical pharmacology of continuous infusion doxorubicin. Ther Drug Monit 11:3–9
44. Tan B, Piwnica-Worms D, Ratner L (2000) Multidrug resistance transporters and modulation. Curr Opin Oncol 12:450–458

45. Tranchand B, Catimel G, Lucas C, Sarkany M, Bastian G, Evene E, Guastalla JP, Negrier S, Rebattu P, Dumortier A, Foy M, Grossin F, Mazier B, Froudarakis M, Barbet N, Clavel M, Ardiet C (1998) Phase I clinical and pharmacokinetic study of S9788, a new multidrug-resistance reversal agent given alone and in combination with doxorubicin to patients with advanced solid tumors. Cancer Chemother Pharmacol 41:281–291
46. Troconiz IF, de Alwis DP, Tillmann C, Callies S, Mitchell M, Schaefer HG (2000) Comparison of manual versus ambulatory blood pressure measurements with pharmacokinetic-pharmacodynamic modeling of antihypertensive compounds: application. Clin Pharmacol Ther 68:18–27
47. Van Zuylen L, Sparreboom A, van der Gaast A, van der Burg ME, van Beurden V, Bol CJ, Woestenborghs R, Palmer PA, Verweij J (2000) The orally administered P-glycoprotein inhibitor R101933 does not alter the plasma pharmacokinetics of docetaxel. Clin Cancer Res 6:1365–1371
48. Wacher VJ, Wu CY, Benet LZ (1995) Overlapping substrate specificities and tissue distribution of cytochrome P4503A and P-glycoprotein: implications for drug delivery and activity in cancer chemotherapy. Mol Carcinog 13:129–134
49. Wade JR, Beal SL, Sambol NC (1994) Interaction between structural, statistical and covariates models in population pharmacokinetic analysis. J Pharmacokinet Biopharm 22:165–177
50. Wang GX, Wang YX, Zhou XB, Korth M (2001) Effect of doxorubicinol on excitation-contraction coupling in guinea pig ventricular myocytes. Eur J Pharmacol 423:99–107